Quantum states of hydrogen atom motion on the Pd(111) surface and in the subsurface

2007 J. Phys.: Condens. Matter 19 365214

(http://iopscience.iop.org/0953-8984/19/36/365214)

IOP PUBLISHING JOURNAL OF PHYSICS: CONDENSED MATTER

J. Phys.: Condens. Matter **19** (2007) 365214 (11pp) doi:10.1088/0953-8984/19/36/365214

Quantum states of hydrogen atom motion on the Pd(111) surface and in the subsurface

Nobuki Ozawa[1], Nelson B Arboleda Jr[1,2], Tanglaw A Roman[1], Hiroshi Nakanishi[1], Wilson A Diño[2,3,4] and Hideaki Kasai[1]

[1] Department of Precision Science & Technology and Applied Physics, Osaka University, Suita, Osaka, 565-0871, Japan
[2] Physics Department, De La Salle University, Manila 1004, The Philippines
[3] Department of Physics, Osaka University, Toyonaka, Osaka 560-0043, Japan
[4] Center for the Promotion of Research on Nanoscience and Nanotechnology, Osaka University, Toyonaka, Osaka 560-8531, Japan

Received 22 February 2007, in final form 13 July 2007
Published 24 August 2007
Online at stacks.iop.org/JPhysCM/19/365214

Abstract

We investigate the quantum states of hydrogen atom motion on Pd(111) surface and in its subsurface by calculating the wavefunctions and the eigenenergies for hydrogen atom motion within the framework of the variation method on an adiabatic potential energy surface (PES), obtained through first-principles calculations, for the hydrogen atom motion. The calculated results show that the ground-state wavefunction for the hydrogen atom motion localizes on the face-centered cubic (fcc) hollow site of the surface. The higher excited state wavefunctions are distributed between the first and second layers, and subsequently delocalized under the second atom layer. These suggest that an effective diffusion path of the hydrogen atom into the subsurface area passes through the fcc hollow site to the octahedral sites in the subsurface. Moreover, activation energies for diffusion of H and D atoms over the saddle point of the PES between the fcc hollow site and the first (second) octahedral site are estimated as 598 (882) meV and 646 (939) meV, respectively. Furthermore, the activation energies for diffusion of H and D atoms over the saddle point of the PES between the first (second) octahedral site and the fcc hollow site are estimated as 285 (483) meV and 323 (532) meV, respectively.

1. Introduction

Paladium (Pd) has drawn much attention as a material with high solubility and permeability for hydrogen and is expected to be one of the promising materials for technological applications in connection with hydrogen storage and purification [1–3]. Many researchers have studied the behavior of hydrogen on the Pd surface and in the subsurface, such as the dissociative adsorption of hydrogen molecules and the diffusion, absorption and associative

desorption of hydrogen atoms through several different approaches for the development of this technology [4–11]. Our previous paper [11] presented an adiabatic potential energy for hydrogen atom motion on the Pd(111) surface and in its subsurface obtained by first-principles calculations to understand how the hydrogen atom behaves after adsorbing on the Pd(111) surface. It is shown that the potential energy for the hydrogen atom motion has a minimum value at the fcc hollow site on the Pd(111) surface and local minima at the hexagonal close-packed (hcp) hollow site on the surface and the octahedral (OH) and tetrahedral (TH) sites in the subsurface. The diffusion path of the hydrogen atom into the bulk starts from the fcc hollow site and passes through the octahedral sites. In discussing the behavior of the hydrogen atom on solid surfaces quantitatively, quantum effects must be considered due to the small mass of the hydrogen atom [12–25]. This paper focuses on the quantum states of the hydrogen (protium: H and deuterium: D) atom motion on the Pd(111) surface and in its subsurface in order to understand the quantum mechanical behavior of the hydrogen atom. The three-dimensional Schrödinger equations for the hydrogen atom motion are solved within the framework of the variation method on the potential energy surface (PES) obtained by first-principles calculations in our previous work [11]. We then discuss the characteristics of the corresponding wavefunctions and eigenenergies. Mainly, we determine the stable states and the effective diffusion path of the hydrogen atom into the subsurface area, and investigate the characters of the quantum mechanical behavior of the H and D atom motion. This paper is organized as follows. Section 2 describes the detail of how the PES and the quantum states are calculated. Section 3 shows our calculation results and discusses the quantum mechanical behavior of the hydrogen atom on the Pd(111) surface and in the subsurface. Section 4 consists of the summary of this work.

2. Theory

2.1. Density functional total energy calculation

The calculations of the adiabatic potential energy for hydrogen atom motion on the Pd(111) surface and in the subsurface have been performed using the density functional method as implemented in the total energy calculation code which solves the Kohn–Sham equations with pseudopotentials and a plane wave basis set, DACAPO [26]. The interactions between the ion cores and the electrons are described by ultrasoft pseudopotentials. All calculations have been performed with the cutoff energy set at 60 Ryd and the two-dimensional Brillouin zone sampled by 16 k-points [27]. Convergence of the total energy has been confirmed. The generalized gradient approximation (GGA) [28] is adopted for the exchange correlation energy. In calculating the PES [11], periodically repeated slabs of five atomic layers are used with a (2×2) unit cell, or with a 0.25 monolayer (ML) H coverage, to set the hydrogen atoms at distances at which the interactions between the hydrogen atoms are minimal. A vacuum of a size equivalent to six atomic layers separates adjacent slabs, and all atoms positions of the slab are fixed. The calculated lattice constant of 3.99 Å for the Pd bulk is in good agreement with the experimental values of 3.89 Å [29]. To obtain the adiabatic PES for the hydrogen atom motion on the Pd(111) surface and in the subsurface, the potential energy calculations are carried out at $12 \times 12 \times 28$ grid points within a unit cell: the 12×12 grid points lie in a plane parallel to the surface within the unit cell and the 28 grid points lie in a line directed perpendicular to the surface, starting from 2.0 Å on the surface to 4.75 Å into the subsurface area at an interval of 0.25 Å. The PES is constructed using three-dimensional spline interpolations in directions parallel and perpendicular to the surface. Here, the origin of the potential energy is set equal to the sum of the total energy of an isolated Pd(111) slab and that of an isolated hydrogen atom.

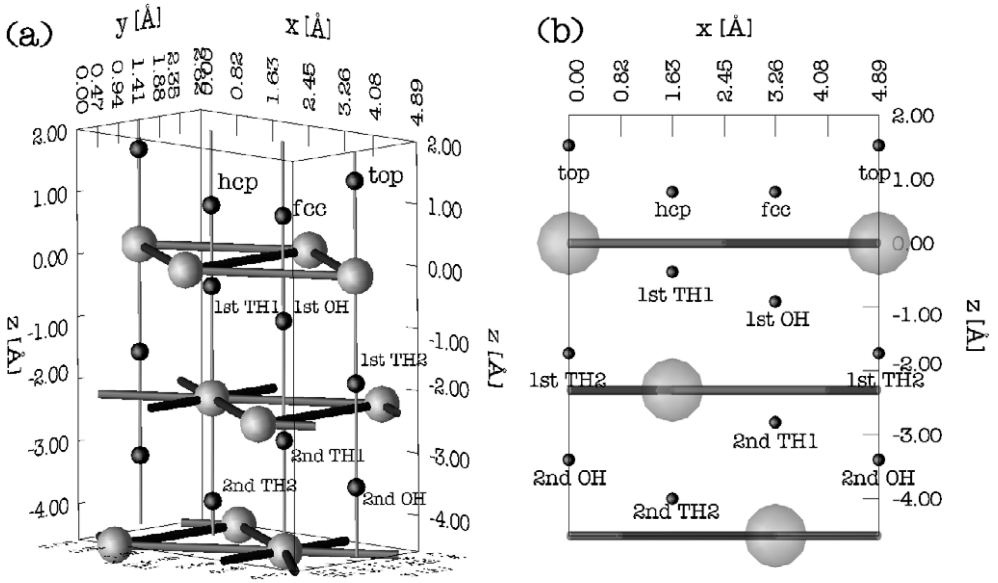

Figure 1. Schematics of specific sites of the Pd(111) surface and subsurface. (a) A bird's eye view and (b) cross-sectional view cutting through the top, hcp hollow, fcc hollow and top sites of the Pd(111) surface. Grey spheres represent the Pd atoms, with the first, second and third layer atoms visually represented. The small black spheres denote the specific sites: top, bridge, hcp, fcc, first (second) OH [the octahedral site between the first and second (second and third) atom layers], first (second) TH1 [the tetrahedral site above the first (second) layer Pd atom], and first (second) TH2 [the tetrahedral site beneath the first (second) layer Pd atom].

2.2. *Wavefunctions and eigenenergies*

Quantum states of the hydrogen atom (H and D) motion are obtained by solving the three-dimensional Schrödinger equation for the hydrogen atom motion on the constructed PES via the variation method [22, 25–27]. Here, periodic boundary conditions are considered along the surface plane. The corresponding wavefunctions for the hydrogen atom motion are constructed with a linear combination of Gaussian-type functions. The Gaussian functions take the following form:

$$\phi_i(x, y, z) = \left(\frac{\beta_x\beta_y\beta_z}{\pi^3}\right)^{1/4} \exp\left\{-\frac{1}{2}[\beta_x(x - X_i)^2 + \beta_y(y - Y_i)^2 + \beta_z(z - Z_i)^2]\right\}, \tag{1}$$

where the index i denotes the Gaussian function whose center is located at the grid point (X_i, Y_i, Z_i). β_x, β_y, and β_z are chosen such that the adjacent Gaussian functions overlap and are half their respective amplitudes at the midpoint of the two functions. Here, β_x, β_y, and β_z are 25.0794 Å^{-2}, 25.0794 Å^{-2} and 138.629 Å^{-2}, respectively. The Gaussian-type functions are located at 8×8 grid points in the direction parallel to the surface and 32 grid points in the direction perpendicular to the surface at intervals of 0.2 Å starting from 1.8 Å on the surface up to -4.4 Å in the subsurface (i.e., up to the third atom layer). The unit cell in the calculations of the quantum states is shown in figure 1. The wavefunctions and the eigenenergies for the ground state, first excited state, second excited state, and so on correspond to the lowest, second lowest, third lowest and so on energy level. The next section presents the results for the case of zero wavevectors in the direction parallel to the surface.

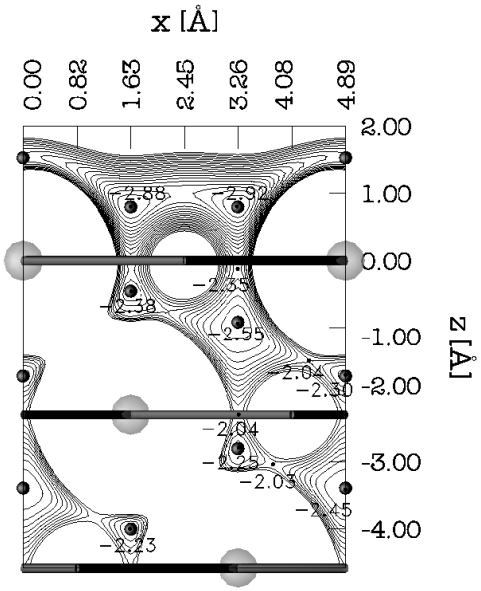

Figure 2. A contour plot of an adiabatic potential energy for hydrogen atom motion on a cross section cutting through the top, hcp hollow, fcc hollow and top sites line. Here, z is the distance from a Pd atomic plane of the surface first layer. x is the surface parallel coordinate along the direction through the top, hcp hollow, fcc hollow and top sites line. Grey spheres and thick black lines denote Pd atoms and Pd atom layers. The contour spacing is 0.1 eV.

3. Results and discussion

3.1. Adiabatic potential energy surface on the Pd(111) surface and in the subsurface

Figure 2 displays the contour plot of the adiabatic PES for the hydrogen atom motion on the Pd(111) surface and in the subsurface on the cross section perpendicular to the surface and cutting through the top, hcp hollow, fcc hollow and top sites line [11]. Here, the PES has a minimum on the fcc hollow site, and has local minima at the hcp hollow, octahedral (OH) and tetrahedral (TH) sites. Saddle points exist at the midpoint of the three neighboring atoms in an atom layer and between the OH site and the TH site. At the saddle point between the fcc hollow site and the first OH site, the potential energy value takes a value of −2.35 eV, as shown in figure 2. Similarly, the potential energy values at the saddle point between the first OH site and first TH2 site, between the first OH site and the second TH1 site, between the second TH1 site and the second OH site and between the first TH2 site and the second OH site are −2.04 eV, −2.04 eV, −2.03 eV and −2.03 eV, respectively. Figure 2 also shows that the adiabatic potential energy for the hydrogen atom motion at the TH site is higher than at the OH site. In addition, the potential energies at the OH and TH sites between the first and second atom layers (first OH and TH sites) are lower than those between the second and third atom layers (second OH and TH sites). Moreover, the characters of the PES show that the intervals of the contour lines around the TH sites are narrower than those around the OH sites, as shown in figure 2, and hence, the gradients of the PES around the TH sites are larger than those around the OH sites. The potential energy values at the high-symmetry sites, summarized in table 1, and these values are in good agreement with the results from other theoretical studies [5, 6].

Table 1. The calculated adiabatic potential energy (PE), eigenenergy (EE) and zero-point energy (ZPE) for H and D atom motion at the localized states on the Pd(111) surface and in the subsurface. The rightmost column gives the ratios of the zero-point energies of the H atom to those of the D atom.

	PE (eV)	EE for H (eV)	EE for D (eV)	ZPE for H (meV)	ZPE for D (meV)	H/D
fcc hollow	−2.92	−2.74	−2.79	179	131	1.37
	−2.91[a]					
	−2.84[b]					
hcp hollow	−2.88	−2.70	−2.75	175	130	1.35
first OH	−2.55	−2.43	−2.47	122	83	1.47
	−2.38[b]					
Second OH	−2.45	−2.34	−2.38	108	68	1.59
First TH1	−2.38	−2.14	−2.19	241	187	1.29
First TH2	−2.30	−2.06	−2.11	243	187	1.30
Second TH1	−2.25	−2.03	−2.07	248	223	1.11
Second TH2	−2.23	−1.97	−2.01	261	220	1.19

[a] Reference [5].
[b] Reference [6].

3.2. Quantum states of hydrogen atom motion

The wavefunctions for hydrogen atom motion on the Pd(111) surface in the ground state and in the first five excited states are shown in figure 3. The ground and first excited state wavefunctions are strongly localized on the fcc and hcp hollow site, respectively as shown in figures 3(a) and (b). The second excited state wavefunction is characterized by a vibrational mode directed perpendicular to the surface and centered at the fcc hollow site. The third and fourth excited state wavefunctions are characterized by vibrational modes directed parallel to the surface as shown in figures 3(d) and (e). Here, the third excited wavefunction is not visible in figure 3(d) since the said wavefunction does not intersect the cross section through top-hcp-fcc-top sites line. The fifth excited state wavefunction is delocalized on the surface as shown in figure 3(f). Figures (c)–(e) show that the eigenenergies whose corresponding wavefunction has parallel vibrational modes are higher than those whose corresponding wavefunction has normal vibrational modes. In order to explain why the parallel-mode energy is higher than that of the vertical mode in this calculation, the gradients of the PES around the fcc hollow site perpendicular to the surface (along the z axis) and parallel to the surface (along the x axis) were calculated. To obtain the gradients of the PES, the harmonic oscillation equation $E(t) = k(t - t_0)^2 + D$ was fitted to the potential energy curves along the x and z axes. Here, t_0 and D are the bottom position and the depth of the potential energy curve, respectively, while k corresponds to the gradient of the potential energy curve. When t_0 and D were adjusted for the potential well perpendicular and parallel to the surface, 1.03 and 1.75 were obtained as the values of the parameter k, respectively. Since vibrational energies are proportional to $\sqrt{k/m}$ (m is hydrogen atom's mass) in the case of the harmonic oscillation approximation, the vibrational energy perpendicular to the surface is then higher than that perpendicular to the surface. However, these calculation results show that the perpendicular mode energy is higher than that of the parallel mode. Other results (i.e., H/Cu(110), [25]) show that the parallel vibrational modes have lower eigenenergies than the perpendicular vibrational modes calculated via the same quantum methods. At present, the reason for such results in this calculation is still under investigation.

At the higher excited states, some wavefunctions show delocalized characters on the surface or the characters of the vibrating mode, with increasing the number of nodes of the

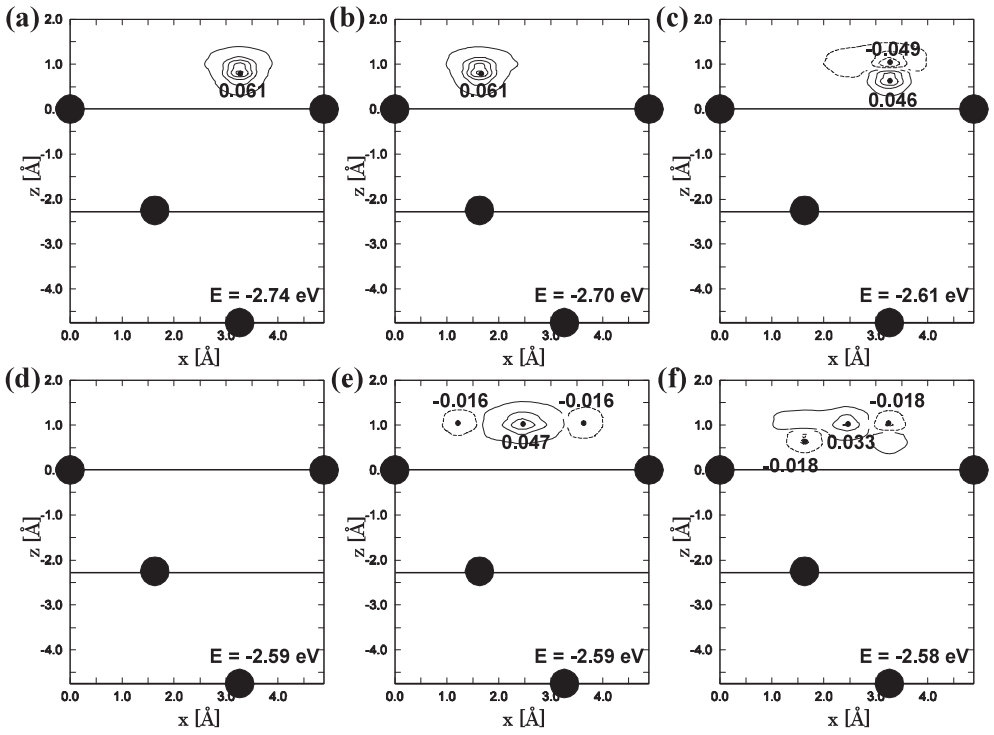

Figure 3. Contour plots of (a) the ground, (b) the first excited, (c) the second excited, (d) the third excited, (e) the fourth excited, and (f) fifth excited state wavefunction for H atom motion on a cross section cutting through the top, hcp hollow, fcc hollow and top sites line. Solid and dashed lines denote positive and negative contours. Here, z is the distance from the Pd atomic plane of the surface first layer. x is the surface parallel coordinate along the direction through the top, hcp hollow, fcc hollow and top sites line. Black spheres and thick black lines denote Pd atoms and Pd atom layers. The contour spacing is 0.015 $\text{Å}^{-3/2}$.

wavefunction in the directions parallel and perpendicular to the surface. Moreover, the excited state wavefunctions show a localized character, as shown in figure 4(a), and vibrational modes parallel and perpendicular to the surface in the subsurface, as shown in figures 4 and 5. The characters of localization in the subsurface are found around the OH and TH sites where the PES takes local minima. Although the wavefunctions for the D atom motion have the same characters as those for the H atom motion, the corresponding eigenenergies for the D atom motion have values different from those for the H atom motion.

3.3. Discussions

The excited energy above the ground state can be compared with the spectrum peaks obtained by high-resolution electron energy loss spectroscopy (HREELS). In HREELS experiments, a scattering electron interacts only with the surface-perpendicular component of the dipole moment of the adsorbed atom [30], and the scattering electron's loss energy corresponds to the vibrational excitation energy. In our results, the third excited state wavefunction for the H atom motion on Pd(111) corresponds to a vibrational mode perpendicular to the surface as shown in figure 3(c). The third excited state energy of the H atom is 134 meV above the ground state, which is in fair agreement with the experiment value of 124 meV observed by HREELS [31].

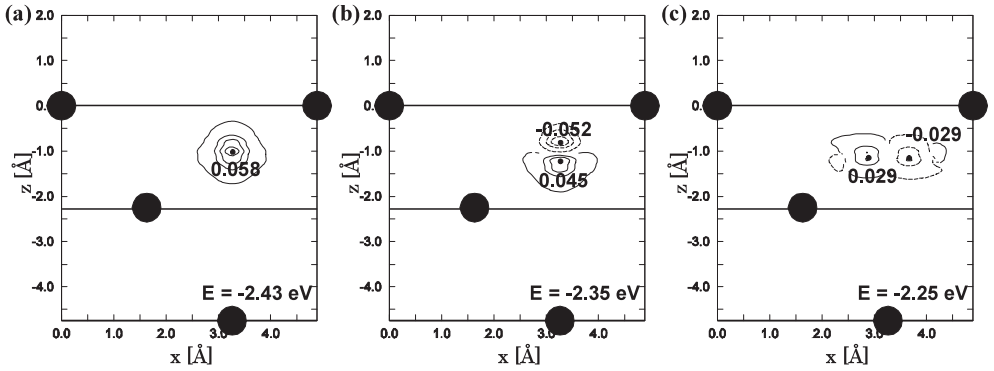

Figure 4. Contour plots of (a) the 19th excited, (b) the 29th excited and (c) the 48th excited state wavefunctions for H atom motion on a cross section cutting through the top, hcp hollow, fcc hollow and top sites line. Solid and dashed lines denote positive and negative contours. Here, z is the distance from the Pd atomic plane of the surface first layer. x is the surface parallel coordinate along the direction through the top, hcp hollow, fcc hollow and top sites line. Black spheres and thick black lines denote Pd atoms and Pd atom layers. The contour spacing is 0.015 $\text{Å}^{-3/2}$.

The localized wavefunctions such as for the ground, the first excited and the 29th excited states have large values compared to the delocalized ones; hence, these states can be considered as intermediate states in the diffusion of the hydrogen atom into the Pd(111) surface in the static state. The eigenenergies and the zero-point energies of the localized wavefunctions are summarized in table 1 and contracted expressions of the symmetry sites follow the figure caption in figure 1. In the last column, the ratios of the zero-point energies of the H atom to those of the D atom all differ from the classical square-root of mass law which shows the difficulty of fitting harmonic oscillations to the PES. While the difference between the potential energy values at the first OH site and first TH1 (TH2) sites is 0.17 (0.25) eV, the difference between the eigenenergies at the first OH site and first TH1 (TH2) sites is 0.29 (0.37) eV, as shown in table 1. This is also the case for the second OH site and second TH sites, as well. Hence, it is clear that the static state at which the hydrogen atom exists at the TH sites becomes much less stable than the state at which the hydrogen atom exists at the OH sites in the calculation via the quantum method. This can be explained as follows. As mentioned in section 3.1, and as shown in figure 2, the gradient of the PES around the TH site is larger than at the OH site. Since the range of the hydrogen atom motion is narrow in a high-gradient region of the PES, the zero-point energy becomes higher due to the quantum uncertainty. It follows that the zero-point energy at the TH site is larger than at the OH site and that the eigenenergy at the TH site is consequently much higher than that at the OH site. Thus, the OH sites should be considered as the intermediate states in the effective diffusion of the hydrogen atom into the subsurface area of Pd.

Figures 5(a) and (b) show the delocalized wavefunction for the H atom motion from the fcc hollow site to the first OH site at the energy value of −2.14 eV and from the first OH site to the second OH site at the eigenenergy of −1.86 eV. In addition, figures 5(c) and (d) show that the wavefunctions for the D atom motion are distributed from the fcc hollow site to the first OH site at the energy value of −2.14 eV and from the first OH site to the second TH1 site and the second OH site at the eigenenergy of −1.85 eV. These excited states are selected as the states with the minimum eigenenergy in the wavefunctions, which are distributed from the fcc hollow site to the first OH site or from the first OH site to the second OH site with a comparatively large value. According to figures 5(a) and (c), the effective diffusion path of the

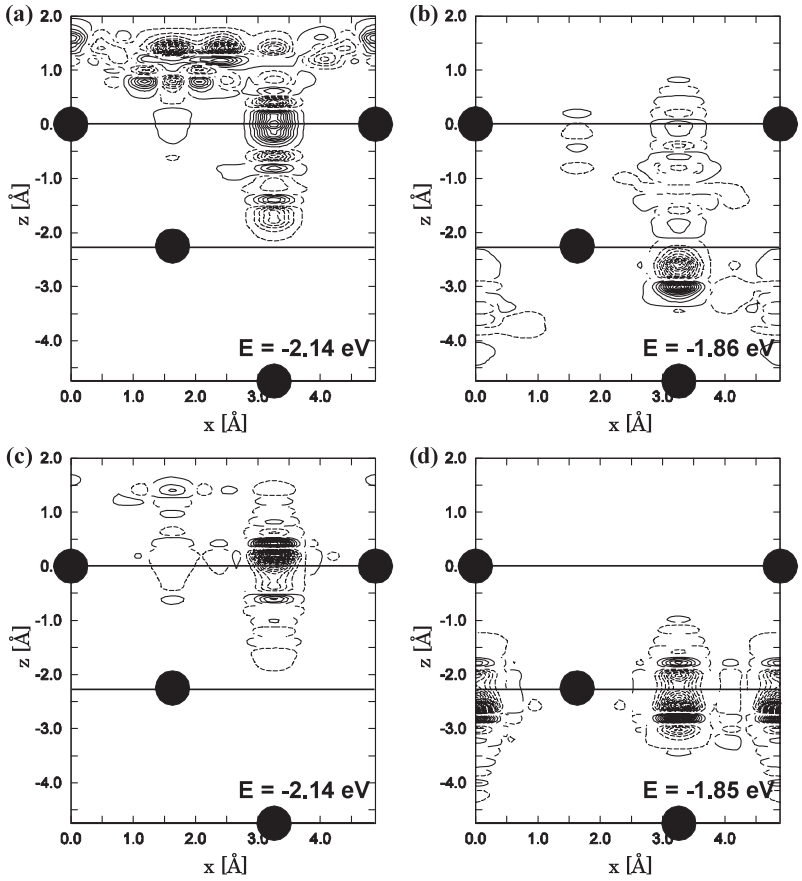

Figure 5. (a) A contour plot of the wavefunction for the H atom motion on a cross section cutting through the top, hcp hollow, fcc hollow and top sites line distributed from the area on surface to the first OH site. Solid and dashed lines express the positive and negative value of the wavefunction, respectively. (b) Same as (a) but for the wavefunction distributed from the first OH site to the second subsurface area. (c) Same as (a) but for the D atom. (d) Same as (b) but for the D atom. Solid and dashed lines denote positive and negative contours.

hydrogen atom passes through the fcc hollow and first OH site over the classical energy barrier between the fcc hollow site and the first OH site. Subsequently, the path distributes from the first OH site to the second OH site, as shown in figures 5(b) and (d). Here, no wavefunctions at the lower excited states, which are distributed from the first OH site to the second TH1 site, are found. Moreover, when the wavefunctions are distributed from the first OH site to the second OH site, those wavefunctions pass at the second TH1 site at the same time. In addition, since the wavefunctions are not distributed to the area on the surface, the diffusion of the hydrogen atoms to the surface in this state is unlikely.

Figure 6 summarizes the energy levels of the H atom motion of which the wavefunctions have the characters of localization at the fcc hollow site and at the OH site and delocalization as shown in figure 5. This energy diagram is described with the adiabatic potential energy curves for the hydrogen atom motion along the diffusion path passing through the fcc hollow site, first OH site, first TH2 and second OH site. The activation energy for diffusion can be determined from figure 6. For example, the activation energy of the H atom from the fcc hollow site to the

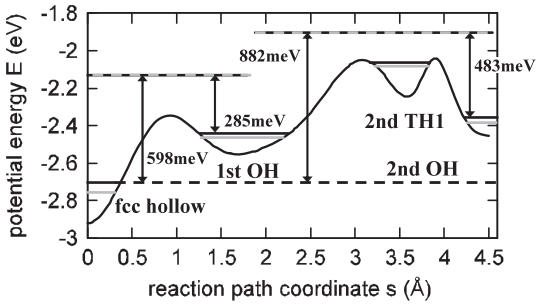

Figure 6. Energy diagram of the eigenenergies for H and D atom motion and the adiabatic potential energy curve as a function of the reaction path coordinate *s*, passing through the fcc hollow, first OH, first TH2 and second OH sites. The origin of *s* is taken from the equilibrium coordinate of the hydrogen atom at the fcc hollow site. Black and grey solid lines denote the eigenenergy for the H and D atom motion, respectively.

Table 2. Activation energies of the H and D atoms from the fcc hollow site to the first (second) OH site and from the first (second) OH sites to the fcc hollow site on the Pd(111) surface and in the subsurface.

	Activation energy for H (meV)	Activation energy for D (meV)
From fcc to first OH	598	646
From first OH to fcc	285	323
From fcc to second OH	882	939
From second OH to fcc	483	532

first OH site is defined as the difference of the eigenenergy value between the ground state of which corresponding wavefunction is localized on the fcc hollow site, and the excited state of which the corresponding wavefunction is distributed from the fcc hollow site to the first OH site, as shown in figure 5(a). Then, table 2 shows the activation energy for the H and D atom diffusion for diffusion paths passing from the fcc hollow site to the first OH site, from the first OH site to the fcc hollow site, from the fcc hollow site to the second OH site and from the second OH site to the fcc hollow site. The activation energy for the H and D atom diffusion from the fcc hollow site to the first (second) OH site is 598 (882) meV and 646 (939) meV, respectively. In addition, the activation energy for the H and D atom diffusion from the first (second) OH site to the fcc hollow site is 285 (483) meV and 323 (532) meV, respectively. The activation energies for the D atom diffusion are larger than the ones for the H atom motion in general, as shown in table 2. For diffusion into the subsurface area, the difference between the eigenenergies for the H atom motion and for the D atom motion, at which the corresponding wavefunctions are delocalized from the fcc hollow site to the first OH site or from first OH site to the second OH site, is very small. In addition, the zero-point energy at the initial site for the H atom motion is higher than the one for the D atom, as mentioned above. Thus, the difference of the eigenenergy for the H atom motion between the fcc hollow site and the first OH site and between the first OH site and the second OH site is larger than that for the D atom motion.

The difference between the potential energy value at the fcc hollow site (−2.92 eV) and at the saddle point of the PES between the fcc hollow site to the first OH site (−2.35 eV) is the value of the classical diffusion barriers between the fcc hollow site and the first OH site (0.57 eV). Similarly, the values of the classical diffusion barriers between the fcc hollow sites and the second OH sites, between the first OH site and the fcc hollow site and between

the second OH site and the fcc hollow site are 0.88 eV, 0.20 eV and 0.41 eV, respectively. Comparing the activation energies with the classical diffusion barriers, it is found that all of the activation energies are larger than the classical diffusion barriers. The experimental data [32] show that the activation energy for the H atom is 0.20–0.23 eV in the Pd bulk, while our calculations show that the classical energy barrier is 0.41 eV and the activation energy is 0.48 eV for the effective diffusion in to the subsurface. Although the systems of the experiment and our study are different, our calculated values are still too high compared with the experimental values owing to the rough assumptions we employed in our calculations. The discrepancy may decrease when the relaxation of the atom layers or tunnel diffusion are considered. Nevertheless, the rough features of the behavior of the hydrogen atom on the Pd(111) surface and in its subsurface described in this study will be useful for the full elucidation of the diffusion mechanism of the hydrogen atom in the future.

4. Summary

We studied the quantum states of hydrogen atom motion on the Pd(111) surface and in the subsurface by calculating the wavefunctions and the eigenenergies for the H and D atom motion using the variation method based on the adiabatic potential energy surface obtained by first=principles calculations. The results show that the ground state wavefunction for the hydrogen atom motion is localized on the fcc hollow site and that the wavefunctions at other sites where the adiabatic potential energy for the hydrogen atom takes a local minimum are also localized. At the higher excited states, the wavefunctions for the hydrogen atom motion are distributed from the fcc hollow site to the first OH site and are subsequently delocalized from the first OH site to the subsurface area between the second and third atom layers. According to the wavefunctions and eigenenergies, the effective diffusion path for the hydrogen atom into the subsurface obtained in this study is determined to pass from the fcc hollow site to the first OH site and subsequently from the first OH site to the second OH site. In the diffusion between the first OH site and the second OH site, the diffusion of the hydrogen atoms to the Pd(111) surface is unlikely. The corresponding activation energy value of the H and D atom over the diffusion barrier at the saddle point of the PES from the fcc hollow site to the first (second) OH site is estimated as 598 (882) meV and 646 (939) meV, respectively, while that from the first (second) OH site to the fcc hollow site is 285 (483) meV and 323 (532) meV, respectively.

Acknowledgments

This work is partly supported by the Ministry of Education, Culture, Sports, Science and Technology of Japan (MEXT), through their Special Coordination Funds for the 21st Century Center of Excellence (COE) program (G18) ‘Core Research and Advance Education Center for Materials Science and Nano-Engineering’ and through their Grants-in-Aid for Scientific Research on Priority Areas (Developing Next Generation Quantum Simulators and Quantum-Based Design Techniques), by Japan Society for the Promotion of Science (JSPS) through their Grants-in-Aid for Scientific Research (A), 19206007, 2007, and by the New Energy and Industrial Technology Development Organization (NEDO), through their program on ‘Research and Development of Polymer Electrolyte Fuel Cell Systems’. Some of the calculations presented here were performed using the computer facilities of Cyber Media Center (Osaka University), the Institute of Solid State Physics (ISSP) Super Computer Center (University of Tokyo), the Yukawa Institute (Kyoto University), and the Japan Atomic Energy Research Institute (ITBL, JAERI).

References

[1] Steele B C H and Heinzel A 2001 *Nature* **414** 315
[2] Li Q, He R, Gao J, Jensen J O and Bjerrum N J 2003 *J. Electrochem. Soc.* **150** A1599
[3] Uemiya S, Kato W, Uyama A, Kajiwara M, Kojima T and Kikuchi E 2001 *Sep. Puirf. Tech.* **22** 309
[4] Christmann K 1988 *Surf. Sci. Rep.* **9** 1
[5] Dong W, Ledentu V, Sautet Ph, Eichler A and Hafner J 1998 *Surf. Sci.* **411** 123
[6] Lovvik M and Olsen R A 1998 *Phys. Rev.* B **58** 10890
[7] Wilde M, Matsumoto M, Fukutani K and Aruga T 2001 *Surf. Sci.* **482–485** 346
[8] Mitsui T, Rose M K, Fomin E, Ogletree D F and Salmeron M 2003 *Surf. Sci.* **540** 5
[9] Nobuhara K, Kasai H, Diño W A, Nakanishi H and Okiji A 2003 *Japan. J. Appl. Phys.* **42** 4630
[10] Nobuhara K, Kasai H, Dino W A and Nakanishi H 2004 *Surf. Sci.* **566–568** 703
[11] Ozawa N, Arboleda N B Jr, Roman T A, Nakanishi H, Diño W A and Kasai H 2007 *J. Appl. Phys.* **101** 123530
[12] Puska M J and Nieminen R M 1985 *Surf. Sci.* **157** 413
[13] Brenig W, Kuchenhoff S and Kasai H 1990 *Appl. Phys.* A **51** 115
[14] Kasai H and Okiji A 1993 *Surf. Sci.* **283** 233
[15] Mattsson T R, Wahnström G and Bengtsson L 1997 *Phys. Rev.* B **56** 2258
[16] Diño W A, Kasai H and Okiji A 2000 *Prog. Surf. Sci.* **63** 63
[17] Bae C, Freeman D L, Doll J D, Kresse G and Hanfer J 2000 *J. Chem. Phys.* **113** 6926
[18] Ke X and Kramer G J 2002 *Phys. Rev.* B **66** 184304
[19] Bădescu S C, Jacobi K, Wang Y, Bedurftig K, Ertl G, Salo P, Ala-Nissila T and Ying S C 2003 *Phys. Rev.* B **68** 205401
[20] Nobuhara K, Kasai H, Nakanishi H and Okiji A 2004 *J. Appl. Phys.* **96** 5020
[21] Arboleda N B Jr, Kasai H, Nobuhara K, Dino W A and Nakanishi H 2004 *J. Phys. Soc. Japan* **73** 745–8
[22] Sundell P G and Wahnström G 2005 *Surf. Sci.* **593** 102
[23] Ozawa N, Roman T A, Nakanishi H, Diño W A and Kasai H 2006 *Surf. Sci.* **600** 3550
[24] Roman T, Nakanishi H, Diño W A and Kasai H 2006 *e-J. Surf. Sci. Nanotech.* **4** 619
[25] Ozawa N, Roman T A, Nakanishi H, Diño W A and Kasai H 2007 *Phys. Rev.* B **75** 115421
[26] Hammer B, Hansen L B and Norskov J K 1999 *Phys. Rev.* B **59** 7413
[27] Monkhorst H J and Pack J D 1976 *Phys. Rev.* B **13** 5188
[28] Perdew J P, Chevary J A, Vosko S H, Jackson K A, Pederson M R, Singh D J and Fiolhais C 1992 *Phys. Rev.* B **46** 6671
[29] Wyckoff W G 1981 *Crystal Structures* 2nd edn (Malabar, FL: Krieger)
[30] Puska M J and Nieminen R M 1985 *Surf. Sci.* **157** 413
[31] Conrad H, Kordesch M E, Stenzel W and Sunjic M 1987 *J. Vac. Sci. Technol.* A **5** 452
[32] Wipf H 1997 *Hydrogen in Metals III* (Berlin: Springer) p 63